The cardenolide UNBS1450 is able to deactivate nuclear factor κB–mediated cytoprotective effects in human non–small cell lung cancer cells

Tatjana Mijatovic,[1] Anne Op De Beeck,[2] Eric Van Quaquebeke,[3] Janique Dewelle,[3] Francis Darro,[3] Yvan de Launoit,[2] and Robert Kiss[1]

[1]Laboratory of Toxicology, Institute of Pharmacy, [2]Laboratory of Virology, Faculty of Medicine, Free University of Brussels; and [3]Unibioscreen S.A., Brussels, Belgium

Abstract

Non–small cell lung cancers (NSCLC) are associated with very dismal prognoses, and adjuvant chemotherapy, including irinotecan, taxanes, platin, and *Vinca* alkaloid derivatives, offers patients only slight clinical benefits. Part of the chemoresistance of NSCLCs results from the constitutive or anticancer drug-induced activation of the nuclear factor-κB (NF-κB) signaling pathways. The present study shows that human A549 NSCLC cells display highly activated cytoprotective NF-κB signaling pathways. UNBS1450, which is a cardenolide belonging to the same class of chemicals as ouabain and digitoxin, affected the expression and activation status of different constituents of the NF-κB pathways in these A549 tumor cells. The modifications brought about by UNBS1450 led to a decrease in both the DNA-binding capacity of the p65 subunit and the NF-κB transcriptional activity. Using the 3-(4,5-dimethylthiazol-2yl)-dephenyltetrazolium bromide colorimetric assay, we observed *in vitro* that UNBS1450 was as potent as taxol and SN38 (the active metabolite of irinotecan) in reducing the overall growth levels of the human A549 NSCLC cell line, and was more efficient than platin derivatives, including cisplatin, carboplatin, and oxaliplatin. The chronic *in vivo* i.p. and p.o. UNBS1450 treatments of human A549 orthotopic xenografts metastasizing to the brains and the livers of immunodeficient mice had a number of significant therapeutic effects on this very aggressive model. [Mol Cancer Ther 2006;5(2):391–9]

Received 9/13/05; revised 10/31/05; accepted 12/1/05.

Grant support: ''Fonds de la Recherche Scientifique Médicale'' (Belgium), the ''Fonds Yvonne Boël'' (Brussels, Belgium), and the ''Région de Bruxelles-Capitale'' (Brussels, Belgium). R. Kiss is a Director of Research with the ''Fonds National de la Recherche Scientifique'' (Belgium).

The costs of publication of this article were defrayed in part by the payment of page charges. This article must therefore be hereby marked advertisement in accordance with 18 U.S.C. Section 1734 solely to indicate this fact.

Requests for reprints: Robert Kiss, Laboratory of Toxicology, Institute of Pharmacy (CP 205/1), Université Libre de Bruxelles, Campus Plaine, Boulevard du Triomphe, 1050 Brussels, Belgium. Phone: 32-47762-2083; Fax: 32-2332-5335. E-mail: rkiss@ulb.ac.be

doi:10.1158/1535-7163.MCT-05-0367

Introduction

Because adjuvant chemotherapy (including camptothecin, taxane, platin, and *Vinca* alkaloid derivatives) has only a limited therapeutic effect, non–small cell lung cancers (NSCLC) are the leading cause of death from cancer in most developed countries, and are characterized by an overall 5-year survival rate as low as 15% (1, 2). Most tumor cells (including NSCLC) are naturally resistant not only to apoptotic-related cell death (type I programmed cell death), but are also resistant to nonapoptotic types such as necrosis, autophagy (type II programmed cell death), senescence, mitotic catastrophe, and paraptosis (3–5). In addition to mechanisms enabling them to resist cell death, NSCLCs are also able to resist various cytotoxic insults because they possess a large set of intracellular signaling pathways that counteract chemotherapeutic insults including the constitutive activation of the phosphatidylinositide-3-kinase (6), Akt (7, 8), and the nuclear factor-κB (NF-κB) signaling pathways (8, 9), all of which are interlinked (8, 10). In fact, the constitutive or drug-induced activation of the NF-κB signaling cascade constitutes one of the major pathways by which tumor cells escape cytotoxic insults (11–13).

NF-κB is a collective designation for a family of highly regulated dimeric transcription factors regulating the expression of genes encoding cytokines and chemokines, factors involved in tumor promotion/proliferation, angiogenesis, and a plethora of antiapoptotic proteins (11–13). Virtually all vertebrate cells express at least one of the five Rel/NF-κB members, p50/p105 (NF-κB1), p52/100 (NF-κB2), c-Rel, p65 (RelA), and RelB, which are assembled into homodimers and heterodimers binding a common DNA sequence motif known as the κB (11–13). The most commonly encountered dimer in mammalian cells is the p65/p50 dimer (11–13). In most normal cells, Rel/NF-κB dimers are retained in the cytoplasm as an inactive complex by means of direct binding with specific inhibitors, i.e., I-κB proteins (11–13). Various signals can lead to the phosphorylation and the subsequent ubiquitin proteasome–mediated degradation of the I-κB proteins with the resultant translocation of the active Rel/NF-κB complex into the nucleus (11–13). In contrast, a large number of tumor cells display constitutively high levels of nuclear NF-κB activity due to the hyperactivation of the NF-κB signaling pathways or to inactivating mutations in the regulatory I-κB subunits (11–13). Experimental data involving NF-κB inhibition/deactivation as an important new approach in the treatment of various malignancies have shown that the transcriptional activation of genes associated with cell proliferation, angiogenesis, metastasis, and the suppression of apoptosis seems to lie at the heart

of the ability of NF-κB to promote oncogenesis and resistance to cancer therapy (13). In our present study, we investigated whether a cardenolide (such as ouabain and digitoxin, belonging to the so-called group of cardiotonic steroids; refs. 14, 15) could deactivate a constitutively activated NF-κB signaling pathway in the experimental A549 NSCLC model. *In vivo* orthotopic xenografts of human A549 NSCLC cells developing in the lungs of immunodeficient mice clearly metastasize into the brains and livers of the host mice and display a broad panel of mechanisms enabling them to resist chemotherapeutic insults including cyclooxygenase-2, prostaglandin E synthetase, ornithine decarboxylase, the lung-related resistance protein, and glutathione S-transferase-α, -μ, and -π (16). The present study clearly shows that A549 NSCLC cells also display a constitutively activated NF-κB signaling pathway. We recently showed that *in vivo*, various compounds used to treat patients with NSCLC (including taxol, irinotecan, and oxaliplatin) are of very limited therapeutic value in the case of the orthotopic A549 NSCLC model (16). We decided to use a cardenolide in order to try to deactivate the NF-κB signaling pathway in A549 tumor cells because (*a*) this type of drug [including digitoxin (17), oleandrin (18), and ouabain (19)] has previously been shown to interfere with the NF-κB pathway, and (*b*) cardenolides have a number of antitumor effects on lung cancers both *in vitro* (20) and *in vivo* (21). The antitumor effects of cardenolides have also been reported for prostate (22, 23) and breast (24) cancers even at the clinical level (25). UNBS1450, the cardenolide used in the present work, is a hemisynthetic derivative of a novel compound (UNBS1244) that we identified in an African plant, *Calotropis procera* (26). Figure 1 illustrates the chemical structure of UNBS1450 and UNBS1244 in comparison with ouabain.

Cardenolides bind to the sodium pump, i.e., Na^+/K^+-ATPase, which is an integral membrane protein found in the cells of all higher eukaryotes and is responsible for translocating sodium and potassium ions across cell membranes with ATP as the driving force (14, 15, 27). Sodium pump activity can be decreased or even inhibited by one class of chemicals only, i.e., the cardiotonic steroids, to which cardenolides belong (27). In addition to pumping ions, the sodium pump interacts with neighboring membrane proteins and organizes cytosolic cascades of signaling proteins to send messages to various intracellular organelles (27, 28). The signaling pathways rapidly elicited by the interaction of cardiotonic steroids with the sodium pump are independent of changes in intracellular Na^+ and K^+ concentrations (27, 28). We have already shown that UNBS1450 reduces the sodium pump activity more markedly than ouabain and digitoxin, and at the same time, is much better tolerated *in vivo* than either ouabain or digitoxin (26).

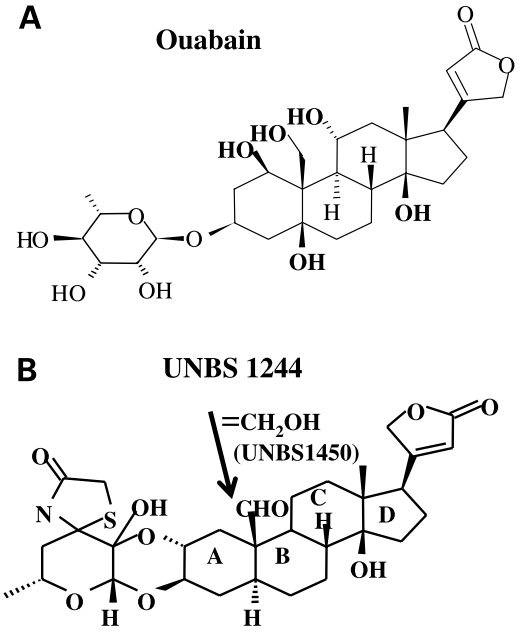

Figure 1. Comparison of the chemical structures of one well-known cardenolide, i.e., ouabain (**A**), with 2″-oxovoruscharin (UNBS1244; **B**) and its hemisynthetic derivative, UNBS1450 (**B**).

Materials and Methods

Compounds

The drugs were purchased as follows: taxol (Paclitaxel; S.A. Bristol-Myers Squibb, Brussels, Belgium), irinotecan (Campto, Aventis, Brussels, Belgium), SN-38 (7-ethyl-10-hydroxycamptothecin; Aventis), oxaliplatin (Oxaliplatin; Inter-Chemical, Ltd., Shen Zhen, China), cisplatin (Platinol; S.A. Bristol-Myers Squibb), carboplatin (Paraplatin; S.A. Bristol-Myers Squibb). The UNBS1450 was obtained by means of chemical hemisynthesis, as detailed elsewhere (26).

Cell Lines

The A549 (ATCC code CCL-185) cell line was obtained from the American Type Culture Collection (Manassas, VA) and was maintained in MEM supplemented with 5% fetal bovine serum, in a mixture of 0.6 mg/mL glutamine (Life Technologies-Invitrogen SA, Merelbeke, Belgium), 200 IU/mL penicillin (Life Technologies-Invitrogen), 200 IU/mL streptomycin (Life Technologies-Invitrogen), and 0.1 mg/mL gentamicin (Life Technologies-Invitrogen). The trypsin-EDTA, the fetal bovine serum, and the cell culture media and their supplements were obtained from Life Technologies-Invitrogen. The fetal bovine serum was heat-inactivated for 1 hour at 56°C. The cells were incubated at 37°C, in sealed (airtight) Falcon plastic dishes (Nunc, Invitrogen SA, Merelbeke, Belgium) in a 5% CO_2 atmosphere.

In vitro Overall Growth Determination

Overall cell growth was assessed by means of the colorimetric 3-(4,5-dimethylthiazol-2yl)-dephenyltetrazolium bromide (Sigma, Bornem, Belgium) assay, as detailed elsewhere (26). The tumor cells were incubated for 72 hours in the presence (or absence – control) of the various drugs. The drug concentrations ranged between 10^{-9} and 10^{-5} mol/L (with a half-log concentration increases). The experiments were carried out in sextuplicate.

Western Blotting Analyses

Cell extracts were prepared by the lysis of subconfluent A549 cells in the SDS-PAGE loading buffer [1× SDS sample buffer, 62.5 mmol/L Tris-HCl (pH 6.8 at 25°C), 2% w/v SDS, 10% glycerol, 50 mmol/L DTT, 0.01% w/v bromophenol blue]. The A549 cell lysates were loaded onto a denaturing polyacrylamide gel (5–12%) and blotted onto a Polyscreen-polyvinylidene difluoride membrane (NEN Life Science Products, Boston, MA). The proteins analyzed (see below) were immunodetected by specific affinity-purified primary antibodies (in TBS containing 0.1% Tween 20 and 5% fat-free dry milk powder or bovine serum albumin) in conjunction with a secondary antibody, in the form of IgG conjugated with horseradish peroxidase. Control experiments included the omission of the incubation step with the primary antibodies (negative control). Equal loading was verified after the Ponceau red coloration of the membranes. The integrity and quantity of the extracts was assessed by means of tubulin immunoblotting. The proteins submitted to Western blotting analyses were detected by means of primary antibodies provided by (*a*) CST Technologies (Westburg, Leusden, the Netherlands): I-κBα (1:1,000), phospho-I-κBα (1:500), ubiquitin (1:500); (*b*) AbCam (Cambridge, United Kingdom): cdc34 (1:500), tubulin (1:3,000); (*c*) BD Transduction Laboratories (Erembodegem, Belgium): p65 (1:500); and (*d*) Santa Cruz (Tebu-Bio, Boechout, Belgium): I-κBβ (1:100). The secondary antibodies used were obtained as follows: anti-mouse and anti-goat IgG from Pierce (PerbioScience, Erembodegem, Belgium), anti-rabbit from NEN Life Science Products, and anti-rat from AbCam. Blots were developed using the Pierce Supersignal Chemiluminescence system (PerbioScience).

NF-κB DNA Binding Assay

NF-κB DNA binding activity was assessed with the Trans-AM NF-κB family transcription factor assay kits (Active Motif Europe, Rixensart, Belgium) developed by Renard et al. (29) as a new sensitive assay to estimate the amount of activated NF-κB in whole-cell protein extracts. This ELISA-like test measures the level of the active form of NF-κB contained in cell extracts specifically able to bind to an oligonucleotide containing the NF-κB consensus site (5′-GGGACTTTCC-3′) attached to a 96-well plate (29). Whole cell lysates were prepared and 10 μg extracts were added to the 96-well plates. The binding of NF-κB to the DNA was visualized by incubation with anti-p50, anti-p52, anti-p65/Rel-A, and anti-Rel-B antibodies that specifically target activated NF-κB, followed by a secondary antibody conjugated with horseradish peroxidase. Antibody binding was determined as absorbance values at 450 nm.

Luciferase Reporter Assay

Although a luciferase reporter plasmid construct (pNF-κB-Luc) containing five NF-κB binding sites was purchased from Stratagene (Amsterdam, the Netherlands), the plasmid construct containing three NF-κB (p3NF-κB-Luc) binding sites was kindly provided by Dr. Corinne Grangette (Laboratoire de Bactériologie des Ecosystèmes, Institut Pasteur, Lille, France). Clones of A549 tumor cells stably containing the NF-κB-Luc constructs were obtained by cotransfection with the NF-κB-Luc plasmid and pSV2neo (30) in a molecular ratio of 10:1. The A549 tumor cells were plated 24 hours after transfection and the isolated clones were selected by cultivating the A549 cells in MEM supplemented with 700 μg/mL of the neomycin analogue G418 (Geneticin, Life Technologies-Invitrogen). Selected A549 clones were analyzed for luciferase activity by the luciferase assay system (Promega, Leiden, the Netherlands). Briefly, 10^4 A549 cells were plated in 96-well plates and, 24 hours after plating (see Results), the cells were cultivated in MEM supplemented with 10 nmol/L UNBS1450 for various experimental times. The cells were rinsed with PBS, lysed in 20 μL of lysis buffer (Promega), and frozen at −20°C. The A549 cell lysates were tested for luciferase activity with 40 μL of luciferase reagent on a TD-20/20 luminometer (Turner Designs, Promega) with an integration time of 30 seconds.

In vivo Orthotopic Grafting of A549 NSCLC Human Cells

The potential *in vivo* UNBS1450-related therapeutic effects were determined on human A549 orthotopic xenografts by administering UNBS1450 chronically by i.p. or p.o. injections thrice a week for 4 consecutive weeks and at different concentrations of the maximum tolerated dose (MTD) varying from (MTD)/32 to (MTD)/8 (see Results). The MTD for UNBS1450 was determined by administering it acutely (i.e., in one single i.p. or p.o. dose) to healthy mice (i.e., not grafted with tumors). The survival periods and the weights of the animals were recorded for up to 28 days after the injection of the compound. Seven different doses of UNBS1450 (i.e., 2.5, 5, 10, 20, 40, 80, 120, and 160 mg/kg) were used to determinate the MTD index. The MTD index is defined as the concentration killing at least one mouse in a group of three after a minimum of 28 days. Acute UNBS1450 MTDs via the i.p. and the p.o. route were 120 and >160 mg/kg, respectively.

As detailed elsewhere (16), orthotopic A549 xenografts were obtained by grafting 2×10^6 human A549 cells through the thorax into the left-hand-side of the lungs of nude mice. All the orthotopic grafts were done under anesthesia [saline; Rompun (Bayer, Leverkusen, Germany); Imalgene (Merial, Lyon, France); 5/1/1, vol/vol/vol]. Highly reproducible tumor developments (100%) were obtained from the A549 tumor grafting in each experiment. The end point of the A549-related experiments was the recording of the survival periods of each of the A549-NSCLC–bearing nude mice. For ethical reasons, each animal was submitted to euthanasia (in a CO_2 atmosphere) when it had lost 20% of its weight as compared with its weight at the time of the tumor graft. As detailed elsewhere, autopsies and histology were done on each mouse to confirm the presence of the tumor development (16). All the *in vivo* experiments described in the current study were done on the basis of authorization no. LA1230509 of the Animal Ethics Committee of the Belgian Federal Department of Health, Nutritional Safety, and the Environment.

Statistical Analyses

Survival analysis was done by using Kaplan-Meier curves and the Gehan generalized Wilcoxon test. All the statistical analyses were carried out using Statistica software (Statsoft, Tulsa, OK).

Results

Human A549 NSCLC Cells Display Constitutively High Levels of NF-κB Activity

Figure 2A shows that A549 tumor cells (*black columns*) display basal RelA/p65 DNA-binding activity as high as in the tumor necrosis factor-α–stimulated Raji cells (*gray columns*) used as the positive control in the colorimetric NF-κB DNA binding assay (29) employed here. High basal levels of NF-κB activity were also observed in stably transfected clones of A549 cells containing three (Fig. 2B) or five (Fig. 2C) NF-κB binding sites in luciferase reporter constructs. The high basal levels of NF-κB activity in A549 tumor cells were further outlined by the fact that TNF-α, one of the most potent NF-κB inducers, less than doubled the NF-κB activity in these A549 cells, even when used at 100 ng/mL (Fig. 2B and C).

UNBS1450 Affects the Expression and Activation Status of NF-κB in Human A549 NSCLC Cells

UNBS1450-mediated effects in connection with expression and phosphorylation status of the different constituents of the NF-κB pathways in the A549 tumor cells were characterized at a 10 nmol/L dose, which, in its turn, constitutes the IC_{50} value in terms of the concentration that reduces the overall growth rate of the A549 cell line by 50% after 3 days of treatment (see below). This dose is at least 100 times lower than the doses reported in other studies whose purpose is to characterize the influences of various cardenolides on the NF-κB signaling pathways (18, 19). The treatment of A549 tumor cells with 10 nmol/L UNBS1450 for 24 hours did not trigger off any cell death processes, a point which was determined by means of flow cytometry (data not shown). We chose to analyze the effects of UNBS1450 over periods as long as 24 hours because we were interested in the ability of this compound to deactivate constitutively activated NF-κB activity and not in its ability to counteract the rapid NF-κB activation resulting from proinflammatory stimulation which occurs within minutes.

Although UNBS1450 (10 nmol/L) was the major factor in inducing the accumulation of I-κBβ in the A549 tumor cells (Fig. 3A), it seemed to leave the levels of expression of I-κBα unchanged (Fig. 3B). In contrast, UNBS1450 decreased I-κBα phosphorylation between 4 and 8 hours following its addition to the A549 tumor cell culture medium (Fig. 3C). UNBS1450 (10 nmol/L) also decreased the levels of expression of cdc34 (Fig. 3D). cdc34 is a ubiquitin-conjugating enzyme (E2) involved in I-κBα ubiquitination and its subsequent proteasomal degradation (31). In addition, 10 nmol/L UNBS1450 also led to a decrease in the accumulation of the βTrCP protein in the A549 tumor cells (data not shown). βTrCP is a ubiquitin ligase (E3) that forms a complex with Skip1 and Cullin1; this complex is involved in I-κBα ubiquitination (32). Furthermore, 10 nmol/L of UNBS1450 induced an increase in the accumulation of ubiquitinylated proteins in the A549 tumor cells by ~8 to 10 hours following its addition to the culture medium of these cells (Fig. 3E). Treatment with MG132, a proteasome inhibitor, was used as a control because proteasome inhibition also results in the accumulation of ubiquitinylated proteins, a feature observed here in the case of MG132 (Fig. 3E).

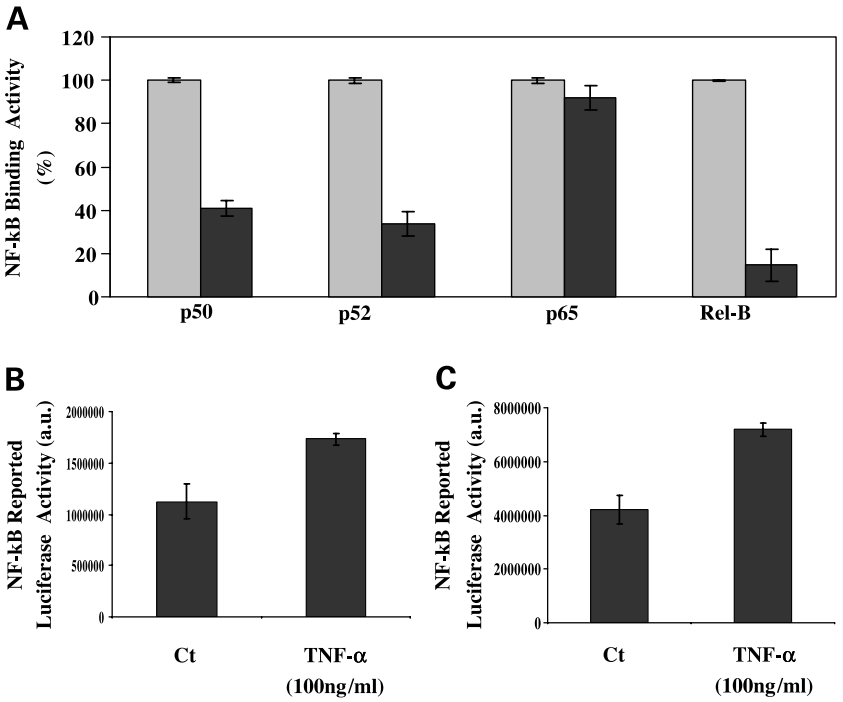

Figure 2. Characterization of the basal NF-κB activity in untreated A549 cells. **A,** characterization by means of the Trans-AM NF-κB family transcription factor assay kit, of the NF-κB DNA binding activity (p50, p52, p65/Rel-A, and Rel-B subunits) in untreated A549 cells (*black columns*) in comparison with TNF-α-treated Raji lymphoblast-like cell extracts (positive control; *gray columns*) arbitrarily normalized to 100%. *Columns,* mean percentages of NF-κB binding activity (*Y* axis); *bars,* ±SE. Each experiment was carried out in triplicate. **B** and **C,** characterization of the NF-κB-dependent luciferase reporter gene expression. A549 tumor cell clones stably transfected with luciferase reporter construct containing either three (**B**) or five (**C**) NF-κB binding sites were left untreated (*Ct*) or treated with 100 ng/mL TNF-α for 6 h. The results are expressed as NF-κB reported luciferase activity (*Y* axis, a.u.). Each sample was assessed thrice. *Columns,* means; *bars,* ±SE.

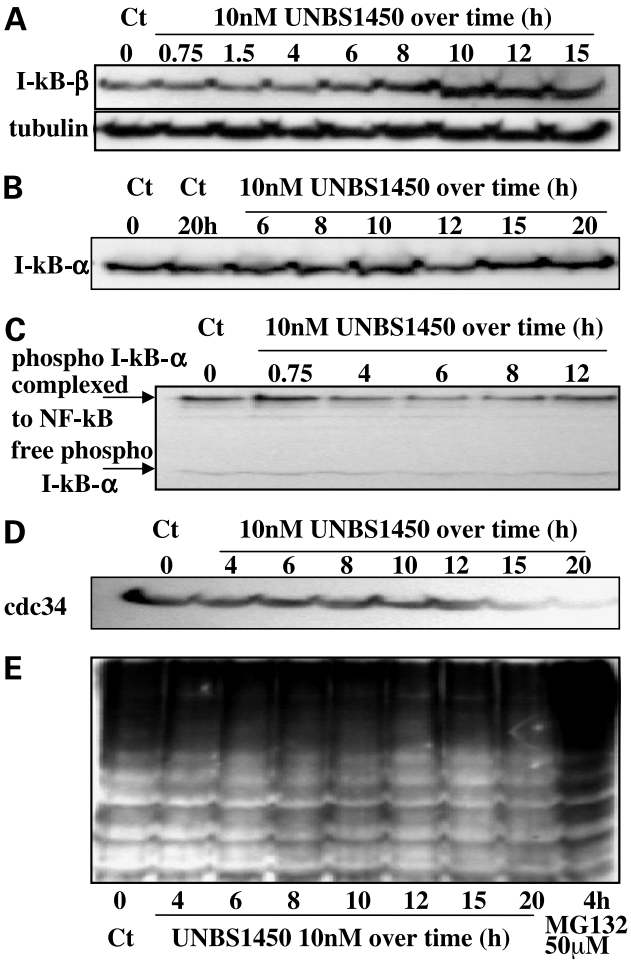

Figure 3. Characterization by means of Western blotting analyses of the 10 nmol/L UNBS1450–mediated effects for a period between 45 min and 12 to 20 h on the expression and phosphorylation levels of the NF-κB inhibitory proteins I-κBβ (**A**) and I-κBα (**B** and **C**). **D**, the effect of 10 nmol/L UNBS1450 treatment on cdc34 protein expression over a period of 20 h. **E**, the effect of 10 nmol/L UNBS1450 treatment on the accumulation of ubiquitinylated proteins in A549 tumor cells, with 50 μmol/L MG132 (a proteasome inhibitor) chosen as a reference.

UNBS1450 Decreased the DNA Binding Capacity of the p65 Subunit

UNBS1450 (10 nmol/L) decreased the levels of the p65/RelA subunit protein accumulation (Fig. 4A). A colorimetric NF-κB DNA-binding assay with cell lysates from untreated and UNBS1450-treated A549 cells at two doses (10 and 100 nmol/L) further revealed that the UNBS1450 treatment of the A549 tumor cells resulted in a dose- and time-dependent decrease in p65 DNA-binding activity (Fig. 4B).

UNBS1450 Decreased the NF-κB Transcriptional Activity

The data in support of an UNBS1450-induced down-regulation of the NF-κB activity presented in Fig. 3 and in Figs. 4A and B were further confirmed by the use of luciferase reporter constructs containing three and five NF-κB binding sites stably transfected into A549 tumor cells (Fig. 4C). Indeed, 10 nmol/L UNBS1450 induced marked time-dependent decreases in the NF-κB reported luciferase activity in the four different A549 tumor cell clones used in the present study.

In vitro Antitumor Effects of UNBS1450 on the Overall Growth of Human A549 NSCLC Cells

UNBS1450 displayed *in vitro* antigrowth activities with respect to the A549 tumor cell populations, similar to those effects observed with taxol or SN38, the active metabolite of irinotecan, but its effects were significantly more pronounced than those observed with various platin derivatives (Fig. 5A).

In vivo Antitumor Effects of UNBS1450 in A549 Orthotopic Xenografts

UNBS1244, the novel cardenolide that we identified in *C. procera*, had an acute MTD level of 10 mg/kg when injected i.p. in healthy mice. This value is similar to those observed with respect to ouabain (5 mg/kg) and digitoxin (10 mg/kg; ref. 26). In sharp contrast, whereas both UNBS1244 and UNBS1450 showed *in vitro* IC_{50} values of ~10 nmol/L with respect to the mean inhibition of the overall growth levels of 57 human cancer cell lines (26), UNBS1450 showed an acute i.p. MTD value of 120 mg/kg. Thus, although UNBS1450 is much better tolerated *in vivo* than its mother compound, UNBS1244, the *in vitro* antiproliferative effects of both compounds are identical.

Orthotopic xenografts of human A549 NSCLCs into nude mice are resistant to taxol and oxaliplatin, and only weakly sensitive to irinotecan (16). However, UNBS1450 markedly increased the survival of A549 NSCLC orthotopic xenograft-bearing mice when given i.p. chronically (12 times) at 10 or 20 mg/kg (Fig. 5B). There are no statistically significant differences between the 10 and the 20 mg/kg dose schedules. Chronic i.p. administrations of UNBS1450 at 5 mg/kg also contributed weak, but nevertheless significant, increases in these survival periods (Fig. 5B). At higher doses, i.e., 40 mg/kg, chronic i.p. treatment was associated with slight toxic effects, i.e., a transient loss of weight in the A549 xenograft-bearing mice, but without the deaths that occurred with a chronic i.p. treatment of 80 mg/kg (data not shown). The experiments illustrated in Fig. 5B were reproduced 6 months later with identical results (data not shown). Furthermore, when chronically administered 12 times p.o. at 80 mg/kg, UNBS1450 was able to bring about a beneficial therapeutic effect in the case of the orthotopic A549 model (Fig. 5C).

One can wonder what happened to A549 orthotopic xenografts *in vivo* following UNBS1450 treatment. Based on the *in vitro* data reported above and on the data relying on an *in vivo* experiment carried out with the s.c. NCI-H727 NSCLC xenograft model, we hypothesize that UNBS1450 decreased the growth rates of both the primary xenografts and brain and liver metastases. Indeed, we treated s.c. NCI-H727 NSCLC xenografts with UNBS1450 exactly as we did here with respect to the A549 NSCLC orthotopic xenograft model: we observed that UNBS1450 decreased by ~50%

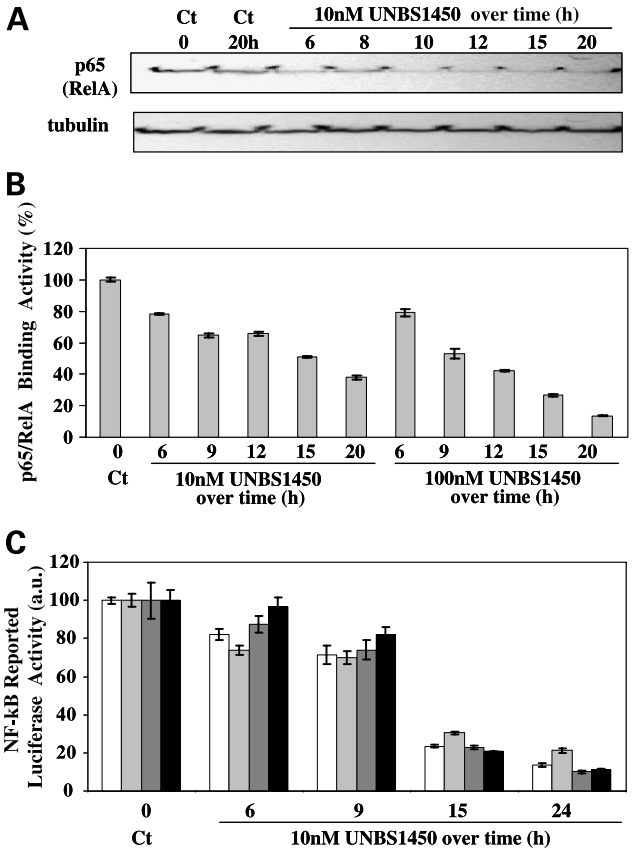

Figure 4. Characterization of the UNBS1450-induced effects on p65/Rel-A protein expression and activity in A549 cells. **A,** Western blotting. The effect of 10 nmol/L UNBS1450 treatment on p65/Rel-A protein expression over a period of 20 h. **B,** characterization by means of the Trans-AM NF-κB family transcription factor assay kit of p65/Rel-A NF-κB DNA binding activity in untreated [control (*Ct*), arbitrarily normalized to 100%], and UNBS1450-treated A549 cells over a period of 20 h. *Columns,* mean percentages of p65 NF-κB binding activity (*Y* axis); *bars,* ±SE. Each experiment was carried out in triplicate. **C,** UNBS1450-induced effects at NF-κB-dependent reporter gene expression level. Three different A549 tumor cell clones stably transfected with the luciferase reporter construct containing five NF-κB binding sites (*open columns, light gray columns*, and *dark gray columns*) and one clone with the luciferase reporter construct containing three NF-κB binding sites (*black columns*) were left untreated (*Ct*), or treated with 10 nmol/L UNBS1450 over a period of 24 h. The results are expressed as percentages of NF-κB reported luciferase activity (*Y* axis) with the untreated control cells set at 100%. Each sample was assessed five times. *Columns,* means; *bars,* ±SE.

the growth rates of the NCI-H727 xenografts at the end of the experiment (data not shown). Experiments are under way in order to characterize the effects of UNBS1450 on the growth rates of brain and liver metastases associated with the orthotopic grafting of the A549 NSCLC xenografts.

Discussion

The signaling pathways that are rapidly elicited by the interaction of cardenolide (including ouabain, whose chemical structure is depicted in Fig. 1) with the sodium pump (and that are independent of changes in intracellular Na^+ and K^+ concentrations) include modifications to the Src kinase, the epidermal growth factor receptor, and the Ras and p42/p44 mitogen-activated protein kinase activity (27, 28), all of which are associated with major roles in biological NSCLC behavior (33–35). In fact, there are two sodium pump pools within the plasma membrane with two different functions, i.e., one being the standard enzyme pool as an energy-transducing ion pump whose partial inhibition by ouabain initiates the increase in intracellular calcium concentration ($[Ca^{2+}]_i$), and the other, the signal-transducing pool of the enzyme, which, through protein-protein interactions, leads to the activation of a signaling intermediate and an increase in the intracellular reactive oxygen species (27, 28). The sodium pump consists of two subunits in equimolar ratios in the shape of α and β subunits, with three α and three β subunit isoforms (27, 28). The levels of the sodium pump α and β subunits can be markedly modified in cancer cells as compared with their normal counterparts (36–38). In fact, it seems that poorly differentiated carcinoma cells show a reduced expression of the β1 sodium pump subunit, a feature that correlates with an increased expression of the Snail transcription factor, which is known to down-regulate E-cadherin (37). In addition, the down-regulation of the β1 sodium pump subunit and E-cadherin by Snail are associated with events leading to epithelial to mesenchymal transition (37), which is an important step in the metastatic processes in lung cancers (39, 40).

The constitutive activation of NF-κB helps a variety of tumors, including NSCLCs, to resist natural or chemotherapeutically induced cell death (11–13). Major efforts to develop NF-κB inhibitors for anticancer purposes are consequently taking place in fundamental research and in the pharmaceutical industry. It is therefore very important to point out the differences in the (de)activation of NF-κB signaling pathways in immune responses and in cancer. Whereas proinflammatory stimuli induce the rapid activation of early response genes, the hyperactivation of the NF-κB signaling pathways in cancers affect the expression of the different genes involved in regulating the ''hallmarks of cancer'' (11–13, 41). Consequently, the mechanisms and their kinetics required for the down-regulation of the NF-κB signaling pathways are different in immune responses and in cancers. As reported in the Introduction, cardenolides are able to deactivate the NF-κB signaling pathways (17, 18) and have a number of antitumor effects on lung cancers (20, 21). In the present study, we clearly show that A549 tumor cells exhibit a high basal level of NF-κB activity, and that UNBS1450 is able to deactivate this NF-κB activity *in vitro* a few hours after the addition of UNBS1450 to the A549 NSCLC cell culture medium. This UNBS1450-induced deactivation of the NF-κB pathways occurs at several levels, including both the inhibitory I-κB portion of the NF-κB signaling pathway and its stimulatory p65/Rel-A NF-κB portion. UNBS1450-induced effects on the inhibitory I-κB protein level involve (*a*) the up-regulation of inhibitory protein expression (as observed for I-κBβ; Fig. 3A), (*b*) the down-regulation of the

phosphorylation levels of I-κBα (Fig. 3C), and (*c*) the down-regulation of the expression of cdc34 (Fig. 3D). The UNBS1450-induced effects at p65/Rel-A NF-κB level include (*a*) the down-regulation of the expression levels of p65 (Fig. 4A), (*b*) the down-regulation of the DNA binding capacity of the p65 subunit (Fig. 4B), and (*c*) the down-regulation of the NF-κB transcriptional activity (Fig. 4C).

The phosphorylation of NF-κB transcription factors is regulated not only by protein serine/threonine kinases, but also by protein serine/threonine phosphatases. Compared with the well-established mechanisms for the phosphorylation of NF-κB transcription factors (that relate to the direct consequence of proinflammatory stimulations, for example), the mechanisms underlying the dephosphorylation of these transcription factors are still poorly understood. Four major classes of protein phosphatases have been described, including PP1, PP2A, PP2B (calcineurin), and PP2C (42). Although PP2B is calcium-dependent, and PP2C is magnesium-dependent, PP1 and PP2A are not dependent on divalent cations (42). PP1 and PP2A are widely expressed in mammalian cells and are involved in the regulation of signaling pathways by a mechanism of phosphorylation/dephosphorylation with a variety of protein kinases (42). Increases in $[Ca^{2+}]_i$ result in the activation of many calmodulin-dependent enzymes such as calcineurin, for example (43). This phosphatase could participate in a site-specific dephosphorylation of I-κBα (phospho-Ser32) resulting in NF-κB deactivation, as is observed in astrocytes (44). Because the interaction of cardenolides with the sodium pump induces an increase in $[Ca^{2+}]_i$ (22), the dephosphorylation of I-κBα observed upon treatment with UNBS1450 (Fig. 3C) could, at least partly, relate to the activation of calcineurin, a feature that we are currently analyzing.

Protein stability is a key regulatory mechanism in the control of cell development, the cell cycle, cell growth and apoptosis, and a recent emerging theme for anticancer drug discovery and development logically relates to protein degradation. The ubiquitin system targets a wide array of short-lived regulatory proteins such as transcriptional activators, tumor suppressors and growth modulators, cell cycle regulators, and signal transduction pathway components (45). Protein degradation by the ubiquitin system involves two steps, i.e., (*a*) the covalent attachment of multiple ubiquitin molecules to the target protein and (*b*) the degradation of the tagged substrate by the 26S proteasome (45). Ubiquitin is covalently attached to substrate proteins by a protein complex usually including an activating enzyme (E1), a conjugating enzyme (E2), and a protein ligase (E3; ref. 45). UNBS1450-induced

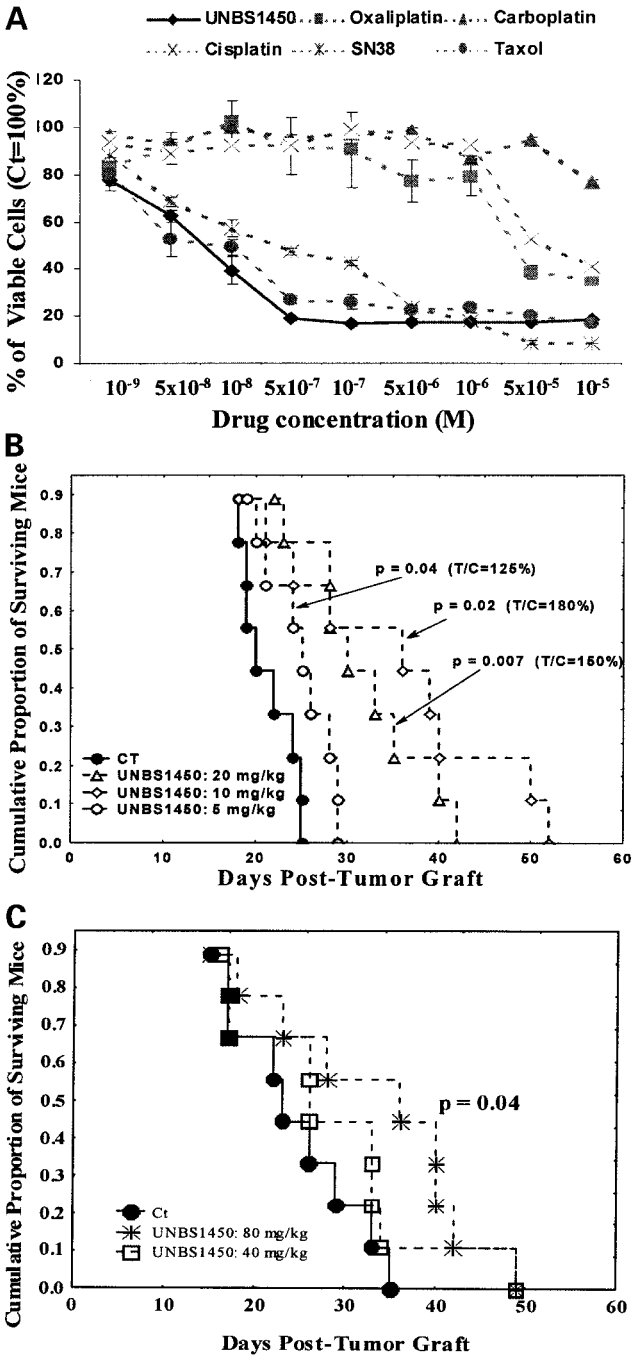

Figure 5. Characterization of UNBS1450-mediated antitumor effects on A549 tumor cells. **A**, characterization of the *in vitro* antitumor effects contributed by UNBS1450 at overall growth levels [monitored by means of the 3-(4,5-dimethylthiazol-2yl)-dephenyltetrazolium bromide colorimetric assay after a 3-d period of treatment] in comparison with taxol, SN-38 (the active metabolite of irinotecan), cisplatin, oxaliplatin, and carboplatin, the five anticancer drugs previously assayed against NSCLCs. The drugs (*X* axis) were assayed at nine concentrations ranging from 10^{-9} to 10^{-5} mol/L with half-log concentration increases; each concentration was analyzed six times. **B** and **C**, illustration of the *in vivo*-mediated UNBS1450 effects on the survival periods of A549 NSCLC orthotopic xenograft-bearing mice. UNBS1450 was assayed i.p (**B**) and p.o. (**C**) thrice a week (on Mondays, Wednesdays, and Fridays) for four consecutive weeks, with the first treatment starting at the 14th day posttumor graft in case of i.p. treatments (**B**) and at the 7th day posttumor graft in case of p.o. administrations (**C**). ●, control mice which received the vehicle. Each experimental group consisted of nine mice.

increases in the level of global ubiquitination therefore suggest that UNBS1450 could affect the ubiquitin-proteasomal protein degradation pathway. Moreover, the levels of expression of cdc34, which is a conjugating enzyme (E2) involved in the degradation pathway of I-κBα, were markedly decreased by UNBS1450 treatment in the A549 tumor cells.

All the effects that we report here with respect to the direct action of UNBS1450 on the cytoprotective effects of the constitutive NF-κB signaling pathways in A549 NSCLC cells are paralleled by marked *in vitro* and *in vivo* antitumor effects on these A549 tumor cells (Fig. 5).

In vitro UNBS1450-induced cell death in the A549 model resulted from a UNBS1450-mediated Hsp70 down-regulation, a process that led to massive caspase-independent tumor cell death involving lysosomal membrane permeabilization (data not shown). Nylandsted et al. (46) already showed cell death processes that occur in relation to modifications in Hsp70 expression. In addition, Frese et al. (47) reported that a selective down-regulation of Hsp70 induces cell death in tumor but not in normal lung cells, a feature that could explain, at least partly, the high therapeutic index observed *in vivo* with respect to UNBS1450.

The potential therapeutic benefit contributed by anticancer drugs could also be eliminated by phosphatidylinositide-3-kinase/Akt signaling pathway. In our study, we observed no *in vitro* additive effects on A549 NSCLC cell mortality when combining UNBS1450 with phosphatidylinositide-3-kinase inhibitors (data not shown), a feature which suggests that the phosphatidylinositide-3-kinase–mediated signaling pathway does not seem to protect NSCLC cells against the UNBS1450-induced cell death–related effects.

Taken together, all these data therefore argue in favor of the use of certain cardenolides to combat a devastating disease like NSCLC. Indeed, apart from the direct antitumor effects evidenced here for UNBS1450 on very aggressive orthotopic xenografts of the human A549 NSCLC model, certain cardenolides could be used to sensitize NSCLC cells to antitumor agents through the deactivation of the cytoprotective effects caused by constitutively activated NF-κB signaling pathways in these tumor cells. In addition, it has already been proved that the enzyme activity or the level of expression of the sodium pump may contribute to the cellular uptake of *cis*-diamminedichloroplatinum(II) and determine the sensitivity of human lung cancer cells to *cis*-diamminedichloroplatinum(II) (48). It has also been proved that the sodium pump is active in both NSCLCs and small cell lung cancers, but that the importance of the enzyme as an active transporter of *cis*-diamminedichloroplatinum(II) may be limited only to NSCLC cells (49). We are currently investigating whether *in vivo* UNBS1450 is capable of improving the antitumor effects of taxol and oxaliplatin on A549 orthotopic xenografts. In parallel, UNBS1450 is entering the candidate drug development stage and should be in phase I clinical trials by 2006.

References

1. Rigas JR. Taxane-platinum combinations in advanced non-small cell lung cancer: a review. Oncologist 2004;9:16 – 23.

2. Gridelli C, Maione P, Airoma G, Rossi A. Selective cyclooxygenase-2 inhibitors and non-small-cell lung cancer. Curr Med Chem 2002;9:1851 – 8.

3. Sperandio S, de Belle I, Bredesen DE. An alternative, nonapoptotic form of programmed cell death. Proc Natl Acad Sci U S A 2000;97:14376 – 81.

4. Okada H, Mak TW. Pathways of apoptotic and non-apoptotic death in tumour cells. Nat Rev Cancer 2004;4:592 – 603.

5. Debatin KM, Krammer PH. Death receptors in chemotherapy and cancer. Oncogene 2004;23:2950 – 66.

6. Lee HY, Srinivas H, Xia D, et al. Evidence that phosphatidylinositol 3-kinase- and mitogen-activated protein kinase kinase-4/c-Jun NH2-terminal kinase-dependent pathways cooperate to maintain lung cancer cell survival. J Biol Chem 2003;278:23630 – 8.

7. Castillo SS, Brognard J, Petukhov PA, et al. Preferential inhibition of Akt and killing of Akt-dependent cancer cells by rationally designed phosphatidylinositol ether lipid analogues. Cancer Res 2004;64:2782 – 92.

8. Mayo MW, Denlinger CE, Broad RM, et al. Ineffectiveness of histone deacetylase inhibitors to induce apoptosis involves the transcriptional activation of NF-κB through the Akt pathway. J Biol Chem 2003;278:18980 – 9.

9. Wiener Z, Ontsouka EC, Jakob S, et al. Synergistic induction of the Fas (CD95) ligand promoter by Max and NFκB in human non-small lung cancer cells. Exp Cell Res 2004;299:227 – 35.

10. Pommier Y, Sordet O, Antony S, Hayward RL, Kohn KW. Apoptosis defects and chemotherapy resistance: molecular interaction maps and networks. Oncogene 2004;23:2934 – 49.

11. Aggarwal BB. Nuclear factor-κB: the enemy within. Cancer Cell 2004;6:203 – 8.

12. Baldwin AS. Control of oncogenesis and cancer therapy resistance by the transcription factor NF-κB. J Clin Invest 2001;107:241 – 6.

13. Nakanishi C, Toi M. Nuclear factor-κB inhibitors as sensitizers to anticancer drugs. Nat Rev Cancer 2005;5:297 – 309.

14. Schoner W. Endogenous cardiac glycosides, a new class of steroid hormones. Eur J Biochem 2002;269:2440 – 8.

15. Dmitrieva RI, Doris PA. Cardiotonic steroids: potential endogenous sodium pump ligands with diverse function. Exp Biol Med (Maywood) 2002;227:561 – 9.

16. Mathieu A, Remmelink M, D'Haene N, et al. Development of a chemoresistant orthotopic human nonsmall cell lung carcinoma model in nude mice. Cancer 2004;101:1908 – 18.

17. Srivastava M, Eidelman O, Zhang J, et al. Digitoxin mimics gene therapy with CFTR and suppresses hypersecretion of IL-8 from cystic fibrosis lung epithelial cells. Proc Natl Acad Sci U S A 2004;101:7693 – 8.

18. Manna SK, Sah NK, Newman RA, Cisneros A, Aggarwal BB. Oleandrin suppresses activation of nuclear transcription factor-κB, activator protein-1, and c-jun NH_2-terminal kinase. Cancer Res 2000;60:3838 – 47.

19. Aizman O, Uhlen P, Lal M, Brismar H, Aperia A. Ouabain, a steroid hormone that signals with slow calcium oscillations. Proc Natl Acad Sci U S A 2001;98:13420 – 4.

20. Kaneda N, Chai H, Pezzuto JM, et al. Cytotoxic activity of cardenolides from *Beaumontia brevituba* stems. Planta Med 1992;58:429 – 31.

21. Inada A, Nakanishi T, Konoshima T, et al. Anti-tumor promoting activities of natural products. II. Inhibitory effects of digitoxin on two-stage carcinogenesis of mouse skin tumors and mouse pulmonary tumors. Biol Pharm Bull 1993;16:930 – 1.

22. McConkey DJ, Lin Y, Nutt LK, Ozel HZ, Newman RA. Cardiac glycosides stimulate Ca^{2+} increases and apoptosis in androgen-independent, metastatic human prostate adenocarcinoma cells. Cancer Res 2000;60:3807 – 12.

23. Yeh JY, Huang WJ, Kan SF, Wang PS. Effects of bufalin and cinobufagin on the proliferation of androgen dependent and independent prostate cancer cells. Prostate 2003;54:112 – 24.

24. Stenkvist B. Cardenolides and cancer. Anticancer Drugs 2001;12:635 – 38.

25. Stenkvist B. Is digitalis a therapy for breast carcinoma? Oncol Rep 1999;6:493 – 6.

26. Van Quaquebeke E, Simon G, Andre A, et al. Identification of a novel cardenolide (2″-oxovoruscharin) from *Calotropis procera* and the hemisynthesis of novel derivatives displaying potent *in vitro* anti-tumor activities and high *in vivo* tolerance: structure-activity relationship analyses. J Med Chem 2005;48:849 – 56.

27. Xie Z, Askari A. Na^+/K^+-ATPase as a signal transducer. Eur J Biochem 2002;269:2434 – 9.

28. Wang H, Haas M, Liang M, et al. Ouabain assembles signaling cascades through the caveolar Na^+/K^+-ATPase. J Biol Chem 2004; 279:17250 – 9.

29. Renard P, Ernest I, Houbion A, et al. Development of a sensitive multi-well colorimetric assay for active NFκB. Nucleic Acids Res 2001;29:1 – 5.

30. Southern PJ, Berg P. Transformation of mammalian cells to antibiotic resistance with a bacterial gene under control of the SV40 early region promoter. J Mol Appl Genet 1982;1:327 – 41.

31. Gonen H, Bercovich B, Orian A, et al. Identification of the ubiquitin carrier proteins, E2s, involved in signal-induced conjugation and subsequent degradation of IκB-α. J Biol Chem 1999;274:14823 – 30.

32. Vuillard L, Nicholson J. Hay RT. A complex containing β-TrCP recruits cdc34 to catalyse ubiquitination of IκB-α. FEBS Lett 1999;455:311 – 4.

33. Haura EB, Cress WD, Chellappan S, Zheng Z, Bepler G. Antiapoptotic signaling pathways in non-small-cell lung cancer: biology and therapeutic strategies. Clin Lung Cancer 2004;6:113 – 22.

34. Janmaat ML, Rodriguez JA, Gallegos-Ruiz M, Kruyt FA, Giaccone G. Enhanced cytotoxicity induced by gefitinib and specific inhibitors of the Ras or phosphatidyl inositol-3 kinase pathways in non-small cell lung cancer cells. Int J Cancer 2006;118:209 – 14.

35. Eberhard DA, Johnson BE, Amler LC, et al. Mutations in the epidermal growth factor receptor and in KRAS are predictive and prognostic indicators in patients with non-small-cell lung cancer treated with chemotherapy alone and in combination with erlotinib. J Clin Oncol 2005;23:5900 – 9.

36. Akopyanz NS, Broude NE, Bekman EP, Marzen EO, Sverdlov ED. Tissue-specific expression of Na,K-ATPase β-subunit. Does β 2 expression correlate with tumorigenesis? FEBS Lett 1991;289:8 – 10.

37. Espinada CE, Chang JH, Twiss J, Rajasekaran SA, Rajasekaran AK. Repression of Na,K-ATPase β1-subunit by the transcription factor snail in carcinoma. Mol Biol Cell 2004;15:1364 – 73.

38. Sakai H, Suzuki T, Maeda M, et al. Up-regulation of Na(+),K(+)-ATPase α 3-isoform and down-regulation of the α1-isoform in human colorectal cancer. FEBS Lett 2004;563:151 – 4.

39. Smythe WR, Williams JP, Wheelock MJ, Johnson KR, Kaiser LR, Albelda SM. Cadherin and catenin expression in normal human bronchial epithelium and non-small cell lung cancer. Lung Cancer 1999;24:157 – 68.

40. Blanco D, Vicent S, Elizegi E, et al. Altered expression of adhesion molecules and epithelial-mesenchymal transition in silica-induced rat lung carcinogenesis. Lab Invest 2004;84:999 – 1012.

41. Hanahan D, Weinberg RA. The hallmarks of cancer. Cell 2000;100: 57 – 70.

42. Mumby MC, Walter G. Protein serine/threonine phosphatases: structure, regulation, and functions in cell growth. Physiol Rev 1993;73: 673 – 99.

43. Hogan PG, Chen L, Nardone J, Rao A. Transcriptional regulation by calcium, calcineurin, and NFAT. Genes Dev 2003;17:2205 – 32.

44. Pons S, Torres-Aleman I. Insulin-like growth factor-I stimulates dephosphorylation of IκB through the serine phosphatase calcineurin (protein phosphatase 2B). J Biol Chem 2000;275:38620 – 5.

45. Glickman MH, Ciechanover A. The ubiquitin-proteasome proteolytic pathway: destruction for sake of construction. Physiol Rev 2002;82: 373 – 428.

46. Nylandsted J, Gyrd-Hansen M, Danielewicz A, et al. Heat shock protein 70 promotes cell survival by inhibiting lysosomal membrane permeabilization. J Exp Med 2004;200:425 – 435.

47. Frese S, Schaper M, Kuster JR, et al. Cell death induced by down-regulation of heat shock protein 70 in lung cancer cell lines is p53-independent and does not require DNA cleavage. J Thorac Cardiovasc Surg 2003;126:748 – 54.

48. Ohmori T, Nishio K, Ohta S, et al. Ouabain-resistant non-small-cell lung-cancer cell line shows collateral sensitivity to *cis*-diamminedichloroplatinum(II) (CDDP). Int J Cancer 1994;57:111 – 16.

49. Bando T, Fujimura M, Kasahara K, Matsuda T. Role of thromboxane receptor on the intracellular accumulation of *cis*-diamminedichloroplatinum (II) in non-small-cell but not in small-cell lung cancer cell lines. Anticancer Res 1998;18:1079 – 84.

Molecular Cancer Therapeutics

The cardenolide UNBS1450 is able to deactivate nuclear factor κB–mediated cytoprotective effects in human non–small cell lung cancer cells

Tatjana Mijatovic, Anne Op De Beeck, Eric Van Quaquebeke, et al.

Mol Cancer Ther 2006;5:391-399.